


Research

Landslide vulnerability mapping using multi-criteria decision-making approaches: in Gacho Babba District, Gamo Highlands Southern Ethiopia

Lemma Tadesse¹  · Abera Uncha¹  · Thomas Toma¹ 

Received: 16 October 2023 / Accepted: 22 January 2024

Published online: 26 January 2024

© The Author(s) 2024 

Abstract

The landslide has been a life-threatening natural disaster in most districts of Gamo Highlands. This study was conducted to assess the status of landslide vulnerability in the Gacho Baba district of the Gamo zone in southern Ethiopia. The Geographic Information System Analytical Hierarchy Process and Weighted Linear Combination multi-criteria decision-making approaches were applied. Eight causative factors of landslide, namely, slope, elevation, aspect, distance from the stream, drainage density, soil type, distance from the road, and land use/cover were considered. The weight values of each causative factor were determined by previous studies, field observations, and experts' judgment. The calculated weight of each causative factor is the slope (23%), elevation (21%), aspect (8%), stream distance and drainage density each (12%), soil type and road length each (9%), and land use/cover (6%). Moreover, the Consistency Index (0.13) and Consistency Ratio (0.08%) were calculated with acceptable values for comparison to weighted overlay analysis to produce a landslide vulnerability map of the study area. The result shows that the vast majority of the study district (86.6%) falls within a very high to moderate landslide susceptibility class and only (13.4%) falls within a very low and low susceptibility. This indicates that almost all the 11 villages in the district, are found within the high to moderate landslide vulnerability class which alerts responsible community and zonal disaster risk prevention and related offices to take action on the identified causative factors to reduce the occurrences of landslide hazard in the study district.

Article Highlights

- The study produced a landslide vulnerability map of the study area and located class based on the magnitude of landslide hazard susceptibility.
- The study pinpoints the importance of incorporating expert knowledge and stakeholder input into the decision-making process to enhance the applicability of the landslide vulnerability mapping results.
- The produced landslide vulnerability of the study area provided valuable information about present and future landslides that is worthwhile for planners and decision-makers for natural resource management

Keywords Analytical-hierarchy process · Causative-factors · Gamo-highlands · Landslide · Vulnerability

✉ Lemma Tadesse, tadesse_lemma@yahoo.com; Abera Uncha, aberauncha@ymail.com; Thomas Toma, thomastoma7@gmail.com |

¹Department of Geography and Environmental Studies, Arba Minch University, Arba Minch, Ethiopia.



1 Introduction

Natural hazards are natural occurrences, processes, or actions that suddenly or violently happen in unusual magnitude and are capable of causing loss of life, injuries to human health, damage to properties, socioeconomic trouble, and environmental degradation [1–4]. Disasters caused by natural hazards have affected 2.5 billion people since 1989 globally and resulted in a loss of 3 trillion dollars economically. The loss has increased from 23 to 150 billion dollars per year since the 1980s for the last decade. The devastating events concentrated mainly in Asia (42%), America (24%), Europe (18%), and Africa (16%), typically due to extreme climatic events [5–7].

According to World Disaster Statistics (2020), landslide hazards cause 13.9% of all catastrophe fatalities globally due to natural disasters in recent decades [8]. Largely due to increased resettlement in landslide-prone areas, as it occurs without warning and does not give people time to leave. [9–11]. Landslide hazards are a heavy burden for regions with rugged terrain and hilly topography [12]. It occurs when the driving force exceeds the resistance due to the instability of the natural soil or rock slope [13]. In addition to rugged terrain and hilly topography, inappropriate land-use planning and construction in mountainous regions also contribute to landslides [14].

In the hilly areas of Eastern Africa, the risk of landslides results in widespread losses of property and human death [15]. The region is highly susceptible to landslides due to its topography, rainfall patterns, and land use changes [16]. Moreover, the lack of comprehensive landslide hazard mapping and monitoring in East Africa led to increased vulnerability to landslide events [1]. The UNDRR [2] has also noted that East African countries are at high risk of landslides and emphasized the need for improved hazard assessment. The Intergovernmental Panel on Climate Change/IPCC/ [17] has also warned climate exacerbates landslide hazards in East Africa, underscoring the urgency for improved risk assessment and management efforts. Despite their significant impact relatively less attention is given to landslide hazards, and related effects in the region [18]. This is not only true for East Africa, but in general, the lack of landslide research in the tropical highlands of Africa compared to other landslide-prone regions globally is striking [19].

In Ethiopia alone, more than 600 locations are identified as landslide hazard-prone [11]. And has become a serious concern to the planners and decision-makers at various levels of the government [20]. However, so far, little effort has been made to reduce losses from such hazards [21]. Its magnitude of occurrence and resulting damage has also increased [22]. Various researchers tried to assess the situations of these occurrences and consequences in different parts of the country such as [8, 10, 11, 13, 21, 23–25] verified that landslide hazards commonly happened in northern, southern, and western highlands of Ethiopia. These areas are further classified into four blocks, namely, block A which represents the northern and northeastern parts of the country. Block B encompasses east and west Gojam and Gondar. Block C represents south and southwestern Ethiopia whereas; Block D constitutes the eastern part of the Main Ethiopian Rift [26].

The present research region is one of those found within block B vulnerable to landslide hazards as highlands make its more than 60% of the Ethiopian terrain [23]. Moreover, according to the information obtained from relevant witnesses, field observations, as well as the researchers' work and field experience, the study area is of natural hazard-prone district, particularly to landslide hazards. Thus, the objectives of this study were (1) to make the inventory of landslide hazards in the study area for examining the status (2) to identify the landslide hazard causative factors and their inter-linkages in the study area context, and (3) to prepare landslide vulnerability map and (4) to classify regions based on the magnitude of landslide hazard susceptibility.

2 Materials and methods

2.1 Description of the study area

Currently, a total of 20 (14 rural and 6 urban) administrative structures are found in the Gamo zone of the Southern Region of Ethiopia. Of these, this research was conducted in the Gacho Baba rural district (Fig. 1). It is part of the Gamo highlands, located between the Abaya-Chamo Lake basins and drained by the Sile and Kulfo watershed tributaries. Astronomically, the district is located between 5° 38' 30" and 6° 10' 50" N latitude and 37° 20' 30" and 37° 31' 30" E longitude. The district is located approximately 541 km south of Addis Ababa, and 36 km from the zonal capital Arba Minch.

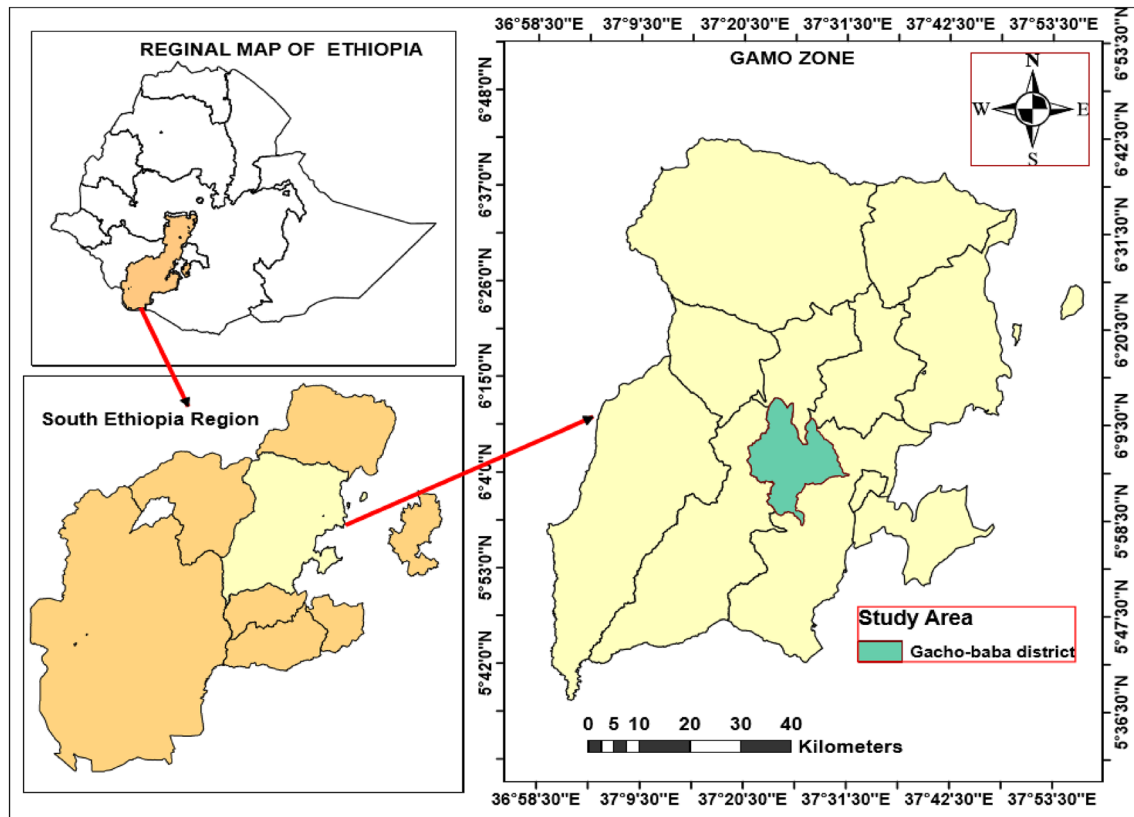


Fig. 1 Locational map of the study area. Source, Ethiopian Central Statistical Agency/CSA/, [28]

2.2 Methods, and materials

Combinations of methods have been applied to come up with landslide vulnerability area assessment and mapping. One of these methods that have been widely used and effective in multi-criteria decision-making (MCDM) is the Analytical Hierarchy Process (AHP) developed by [27]. The reason for using AHP approaches is that it not only provides landslide susceptibility at the time of investigation, but also identifies areas of future very high, high, and moderate potential landslide hazard-prone regions [29]. AHP can also perform landslide susceptibility analysis using relative comparisons of parameters to avoid inconsistencies in the decision-making process and the weight values investigated in landslide vulnerability assessment studies can be scaled up to other regions with similar environmental conditions [16, 24, 30].

The AHP technique is a multi-criteria analysis to build consistent ratings for the variables and helps the user to have the best preference from the alternatives [31]. The rating involves a hierarchical structure by reducing the number of variables into pairwise comparison and developing priorities based on the user's decisions to show the relative importance of the factors [32]. As indicated in Table 2, eight causative factors of landslide in the study area were considered and their weight values were determined using the previous studies, observations made during the land inventory, experts, and physical features of the study area following steps suggested by [27].

1. Producing the pairwise comparison matrix with a value between 1 and 9 was assigned to each causative factor per its relative importance. The scale 1 represents equal importance and 9 refers to extremely important (Tables 1, 4).
2. Construct the normalized pairwise comparison matrix table by dividing each value in the column of the pairwise comparison matrix by the sum of the columns (Table 5).
3. Calculate the weight of each factor by dividing the total of each row in the normalized pairwise comparison matrix table by the total number of factors (Table 6).

Following the computation of weight for each landslide causative factor, the accuracy and consistency of the comparison were checked using the consistency index (CI) equation that is denoted as;

Table 1 The AHP factors comparison scale

Scale	Degree of Preference	Description
1	Equally	Two activities contribute equally
3	Moderately	Experience and judgment slightly to favor one activity
5	Strongly	Experience and judgment strongly favor one activity t
7	Very strongly	One activity is strongly favored over another
9	Extremely	The evidence of favoring one activity over another is of the highest degree possible of an affirmation
2,4,6,8	Intermediate value	Used to represent compromises between the preferences in weights 1,3,5,7 and 9

Source, [27]

$$CI = \frac{\lambda_{max} - n}{n - 1} \quad (1)$$

where, CI refers to the consistency index, 'n' is the number of causative factors, and λ_{max} is the highest eigenvalue of the pairwise comparison matrix. Next, the consistency ratio (CR) was calculated using the following equation (Eq. 2) recommended by [27] which is

$$CR = \frac{CI}{RI} \quad (2)$$

in which, RI represents a consistency index obtained from a simulation runs and varies depending on the order of the matrix. "The CR range varies with the size of the factor's matrix that is (0.05 for 3*3, 0.08 for 4*4, and 1.0 for all larger matrices, $n \geq 5$). A value of $CR \leq 10\%$ indicates a good level of consistency while e a CR value of $> 10\%$ represents the inconsistency of judgments within the matrix". Lastly, thematic map preparation and reclassification were done for each landslide causative factor using the same measurement scale using ArcGIS spatial analyst tools and AHP techniques. The prepared spatial layers were overlaid together in the GIS environment using the weight overlay approach to prepare a landslide susceptibility map of the study area (Eq. 3).

$$w = \sum_{i=0}^n x_i * w_i \quad (3)$$

from Saaty [27] was deployed where 'w' is the weighted overlay, 'n' is the number of decision criteria, 'x_i' is the normalized criterion, and 'w_i' is the respective weight criterion. Finally, the pixel values of the factor layers are multiplied by their percentage to create a landslide susceptibility raster map of the study area.

Besides, multi-temporal satellite images, topographic maps of the district, FAO Digital Soil Map of the World, and the Advanced Spaceborne Thermal Emission and Reflection Radiometer (ASTER) satellite data were the materials used to conduct the analysis (Table 2). Sentinel-2 satellite imagery was used for land use/cover mapping as it is recommendable for land class cover mapping and change detections [33, 44]. Thus, in this project, Sentinel-2 satellite imagery of the acquisition of July 2022 had been used. As the Sentinel-2 satellite images are already georeferenced before at hand, no need for geo-referencing. The geometric registration methods and output Root Mean Square (RMS) error were used to check as it is below 0.5 and after registration; the study area was subset for the areas of study using the district's boundary. The procedure involved the collection of past landslide history of the area from zonal, and district disaster records and local communities, aerial photographs, and satellite images, Field surveys were also utilized to collect valuable information. Once the landslide inventory was completed, statistical and spatial analysis techniques were applied to identify patterns and relationships between various causative factors.

A slope map or digital elevation model of the study area was developed from the ASTER satellite. The soil map was prepared from the FAO soil database map, while the collection of Ground Control Points (GCP) training sites became the past landslide history of the study area, where landslide hazards caused the disasters to happen. As the training data set for supervised classification was developed, a significant number of training sites were identified. To ensure its correctness, the ground truth was consulted on a digital globe, and a base/topographic map of the research region was employed to assess inter-rater reliability for land use and land cover classification. The layers were created for all

Table 2 Respective causative factors and sources of data used for the study

Factors	Description	Sources
FAO Digital Soil Map of the World (DSMW)	Downloaded	https://www.fao.org/soils-portal/data-hub/en/
ASTER satellite for DEM generation with 20-m resolution	Downloaded	https://www.earthdata.nasa.gov/news/new-aster-gdem
Multi-temporal Landsat 8 image with 30 m resolution	Downloaded	https://earthexplorer.usgs.gov/
Slope angle	Developed from DEM 20 M*20 M	DEM 20 M*20 M
Aspect	Developed from DEM 20 M*20 M	DEM 20 M*20 M
Elevation (meter)	Developed from DEM 20 M*20 M	DEM 20 M*20 M
Distance from Stream	Extracted from DEM 20 M*20 M	DEM 20 M*20 M
Distance from Road	Extracted from Google Earth	Topographic maps of the district
Soil type	Derived from FAO Digital Soil Map of the World	FAO Digital Soil Map
Landuse/cover	Derived from Sentinel-2 satellite with 10-m resolution	Esri Inc. published (July 2022)

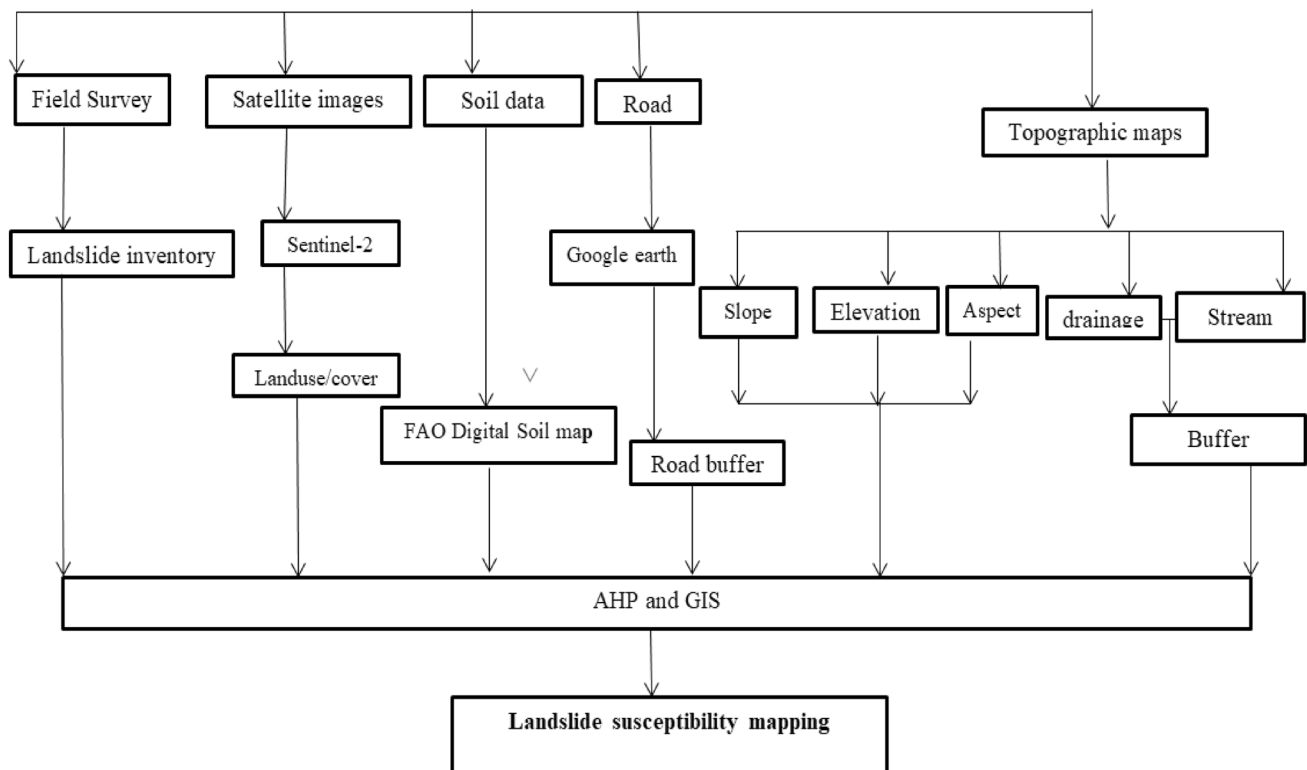


Fig. 2 Flow chart showing the detailed methodology of landslide vulnerability mapping. Source, Prepared by authors (2023)

significant causative and contributing factors that have been identified, and their relationship was statistically examined. Lastly, to construct the landslide vulnerability map, all output layers were blended using weights of factors and sub-factors derived by the AHP approach, and all thematic layers were entered into a GIS environment to identify the research area's landslide susceptibility (Fig. 2).

3 Results

3.1 Landslide causative factors map preparation, and reclassification

The factors that result in land instability are categorized as triggers and predictors [6]. Generally, in Gamo highlands the major triggers are precipitation and human intervention while the predictors are slope, elevation, aspect, distance from the stream, drainage density, soil type, distance from the road, and land use/cover [23]. In the landslide susceptibility analysis, the triggering factors are only taken into account if there is an interest in the time components [32]. As it is only focused on the spatial components, the above-mentioned predictor factors were not considered in this study. Thus, as indicated in (Table 2) the major data for landslide susceptibility and risk assessment were prepared from a variety of sources and compiled into a spatial database. The frequency of landslides in each of these causative factors was calculated as an thematic map and reclassified into the same measurement scale rating from (1–5) based on landslide inventory carried out during field observations using spatial analysis tools of Arc GIS software. To create a landslide vulnerability map, all resulting layers were combined using the factor and sub-factor weights determined by the AHP method consulting with landslide inventory conducted during field observations, local experts, and reviewed literature. The WLC method and AHP results were used to integrate all subject layers into the GIS environment.

3.1.1 Slope factor

The slope steepness is taken into account as one of the major causative factors of the landslide as many factors express the result of its combination effect and the steeper the slope, the tendency for failure will provide other instability [31].

With this consideration, the slope of the study area has been analyzed from the DEM with a resolution of 20 m × 20 m using the (Arc GIS10.4) software and used in research. Researchers have used different classification intervals to show the correlation between slope angle and landslide susceptibility according to the properties of the land, land conditions, and the occurrences of landslides [34]. For this study, considering the occurrences of past landslides [35] landslide Hazard Evaluation Factor (LHEF) rating scheme was employed to develop a slope morphometric class of the study area as escarpment > 45°, steep slope (35–45°), moderately steep slope (25–35°), gentle slope (15–25°) and very gentle slope < 15°. To this end, the reclassified slope map of the study area has indicated that slope ranging (> 45°) and 35–45° which is classified as very high risk and high-risk accounting for 6.54% (1576.2 ha) and 13.83% (3339.2 ha), separately. The areas with moderate, low, and very low comprise 21.91%, 29.02, and 28.68% in their orders (Table 3 and Fig. 3a). Generally, steep slope areas are found in the north, central, and eastern parts of the study district.

3.1.2 Elevation factor

Elevation of an area is among the physiographic factors used for landslide hazard vulnerability analysis [47]. In most cases, highly elevated areas have a higher susceptibility to landslides and elevation plays a significant role in the occurrence of landslides [37]. The altitude of the study area ranging from 1284 to 3493 m is categorized into five levels on its landslide risk classes. The result shows that about 16.2% and 21.56% of the total areas are categorized as very high risk and high risk for landslide hazard, respectively (Table 3 and Fig. 3b).

3.1.3 Aspect factor

In the context of landslide susceptibility, aspect refers to the direction that a slope faces. The aspect of a slope can affect its exposure to sunlight, wind, and precipitation, which can in turn influence the moisture contents and slope stability [25, 31]. According to [32, 38] slopes facing to the east and west, and the southwest and northwest have more relationship with landslides by the area's general physiographic trend and the precipitation direction. This means that slope inclination may behave differently depending on their aspect which may control moisture, seepage, and pore-water pressures [39]. In this study, the aspect morphometric characteristics of the study area (Table 3 and Fig. 3c) were divided into five intervals (west and east, southwest & northwest, southeast and northeast, north and south, and flat) to assign a risk class rating scale based on area's physiographic characteristics.

3.1.4 Distance from the stream

The distance from the stream can affect landslide susceptibility as it is more likely to occur in areas closer to streams [40, 41]. Because the soil in these areas tends to be more saturated and unstable due to the higher water content [8]. The presence of a stream can also increase the erosion rate, which can further weaken the soil and increase the risk of landslides. In addition, streams can act as natural drainage channels, carrying water and debris downhill during heavy rainfall events [40]. Therefore, when assessing landslide susceptibility, it is important to consider both the drainage density and the distance from streams in an area [37]. For this research as with other factors, the stream networks were generated from 20*20 m resolution DEM (Table 3 and Fig. 3d), and Euclidean distance was calculated using the Arc GIS spatial analysis tool. The result indicates the study area is compressed within two watersheds having 44% and 29% belonging to very high and high levels of susceptibility to landslide.

3.1.5 Drainage density

Drainage density is among the factors responsible for landslides. High drainage density can facilitate the susceptibility of an area to landslides increasing erosion and soil saturation [40, 42]. Moreover, as the drainage density becomes high, it can lead to the formation of channels and gullies that function as a pathway for downward movements of debris [38]. Therefore, understanding the drainage density of an area is crucial for identifying areas that are at risk of landslides to implementing appropriate mitigation measures. For this study, the drainage density of the study area was classified into five measurement scales ranging from very high risk to very low (Table 3 and Fig. 4e). The result shows that 6% and 8% of the study areas were categorized as very high and high with the total density of 2.59–3.23 and 1.94–3.23) density of stream total length in respect to its total area respectively.

Table 3 Distribution of study area by Landslide causative factors, susceptibility level, and rating scale

Causative factors	Class	Pixel class	Area		Landslide susceptibility	Rating scale
			(Ha)	(%)		
Slope (degree)	0–15	172,858	6914.32	28.68	Very low	1
	15–25	174,841	6993.64	29.02	Low	2
	25–35	132,050	5282	21.91	Moderate	3
	35–45	83,480	3339.20	13.85	High	4
	>45	39,405	1576.20	6.54	Very high	5
Elevation (Meter)	1284–1742	83,257	3330.28	14.41517	Very Low	1
	1742–2079	135,689	5427.56	23.49329	Low	2
	2079–2405	140,787	5631.48	24.37596	Moderate	3
	2405–2752	124,531	4981.24	21.56138	High	4
	2752–3493	93,301	3732.04	16.1542	Very high	5
Aspect	West and East	119,105	4764.20	19.84	Very high	5
	SW and NW	143,772	5750.88	24.05	High	4
	SE & NE	153,703	6148.12	25.71	Moderate	3
	N & S	116,077	4643.08	19.47	Low	2
	Flat	65,377	2615.08	10.93	Very low	1
Stream distance (Meter)	> 2000	26,844	1073.76	4.420563	Very low	1
	1500 – 2000	41,381	1655.24	6.814458	Low	2
	1000 – 1500	96,622	3864.88	15.91133	Moderate	3
	500 – 1000	174,640	6985.6	28.75902	High	4
	0 – 500	267,766	10,710.64	44.09464	Very high	5
Drainage density (km ²)	0 – 0.67	307,674	12,306.96	54.23977	Very low	1
	0.67 – 1.29	82,018	3280.72	14.45893	Low	2
	1.29 – 1.94	100,374	4014.96	17.69491	Moderate	3
	1.94 – 2.59	45,498	1819.92	8.02083	High	4
	2.59 – 3.23	31,684	1267.36	5.585564	Very high	5
Soil type	Acrisols	27,717	17,738.88	73.05097	Very high	5
	Nit sols	3576	2288.64	9.424912	High	4
	Fluvisols	3351	2144.64	8.831901	Moderate	3
	Lltosols	187	119.68	0.492858	Low	2
	xerosols	3111	1991.04	8.199357	Very low	1
Road distance	0–50	3632	145.28	0.598103	Very high	5
	51–100	3811	152.44	0.62758	High	4
	100–150	3083	123.32	0.507696	Moderate	3
	150–200	3674	146.96	0.60502	Very low	2
	> 200	593,053	23,722.12	97.6616	Low	1
Land use/cover	Forest	99,779	907.76	3.929287	Very low	1
	Rangeland	778,465	7784.65	33.69627	Low	2
	Built up area	36,367	363.67	1.574165	Moderate	3
	Farm Land	1,402,968	14,029.68	60.72821	High	4
	Bare land	1665	16.65	0.07207	Very high	5

NW North West, SE South East, NE North East, N North, S South Source, Reclassified maps

3.1.6 Soil type

The susceptibility of soil to landslides depends on a variety of factors [15]. These are shearing strength, erosion vulnerability, water content, and defined geological and environmental conditions [23]. Soil types are also among contributors and soils such as clay and silt are more prone to landslide as they have a lower shear strength and water content, compared with those with coarse grain that have higher shear strength and less water content [36]. Consequently, considering the soil type and its properties is important in judging the landslide susceptibility of an area. As indicated in Table 3 and Fig. 4f,

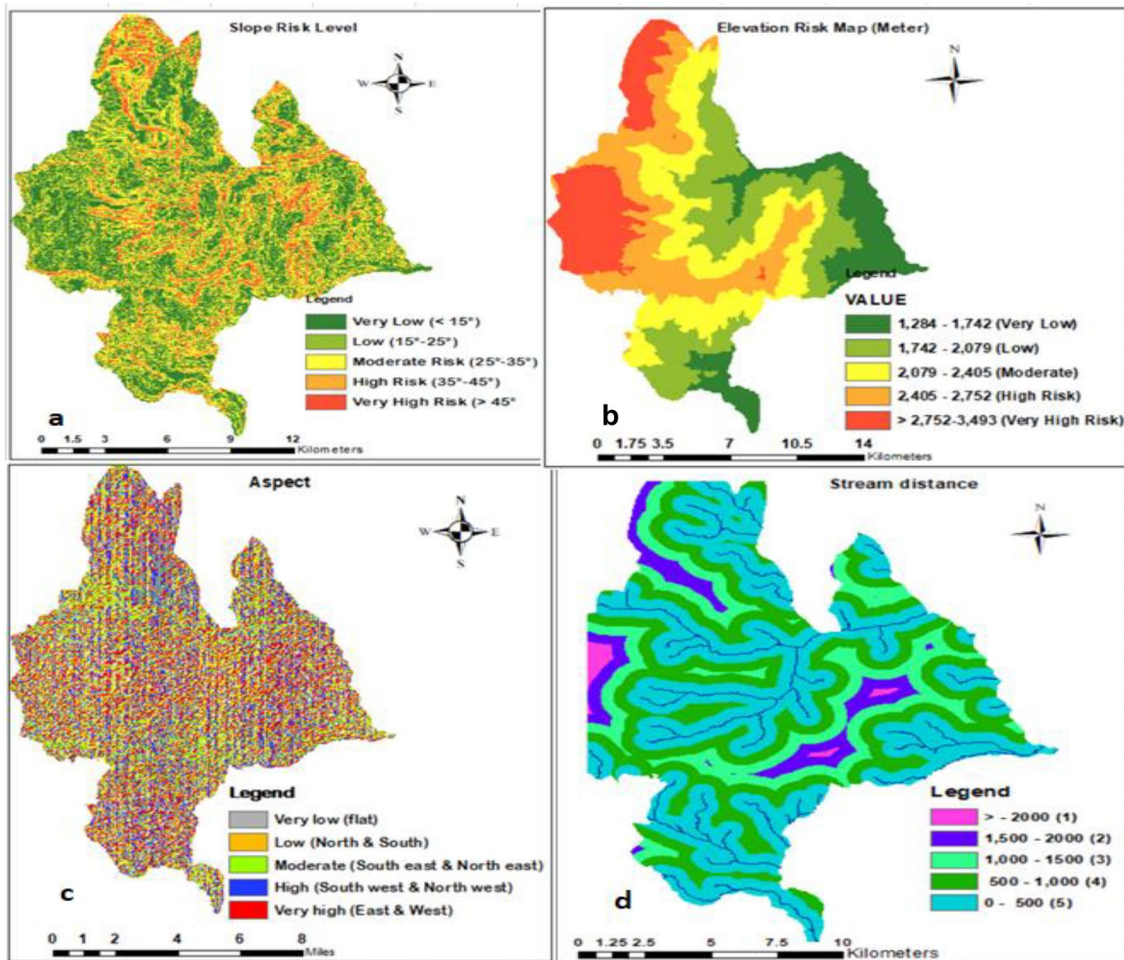


Fig. 3 Slope **a**, elevation **b**, aspect **c**, and stream distance **d** Source, Generated from DEM of the study area

soil types of the study area are reclassified into five categories (Acrisols, nit sols, fluvisols, litosols, and calcic xerosols) and the majority of the area is occupied by Acrisols (73%). Acrisols are among soil types commonly found in highland areas characterized by low levels of organic matter and are highly prone to landslide hazards because of delayed infiltration [26]. Thus, possible to conclude that soil type is among the contributing factors for landslide hazard that has been and will also continue to be a causative factor for landslide hazard susceptibility in the study area.

3.1.7 Road distance

Road construction can contribute to the landslide susceptibility of an area as it results in the cutting of hills and alters the natural drainage pattern of an area which can increase the likelihood of landslides. The construction of roads also increases access to human activities in landslide-prone areas which can further destabilize the soil and increase the risk of landslides [18, 37, 43, 47]. As observed during the fieldwork in January 2021, the main road crosses the study area at a buffer of 0–50 m (Table 3 and Fig. 4g) which contributes to the occurrence of landslide susceptibility.

3.1.8 Landuse/cover

Land use and land cover are among the main factors contributing to landslide susceptibility [25]. In barren and sparsely vegetated lands, landslide activity becomes high because of relatively high weathering, erosion, and other activities [31]. Land use/cover has also an impact on the strength of slope materials against sliding and control of water content [18]. The landuse/cover of the study area was derived from Sentinel-2 satellite 10 m resolution at the acquisition date of July 2021 (Table 2) and classified into five class covers controlling the training pixels with the help of Google Earth, field

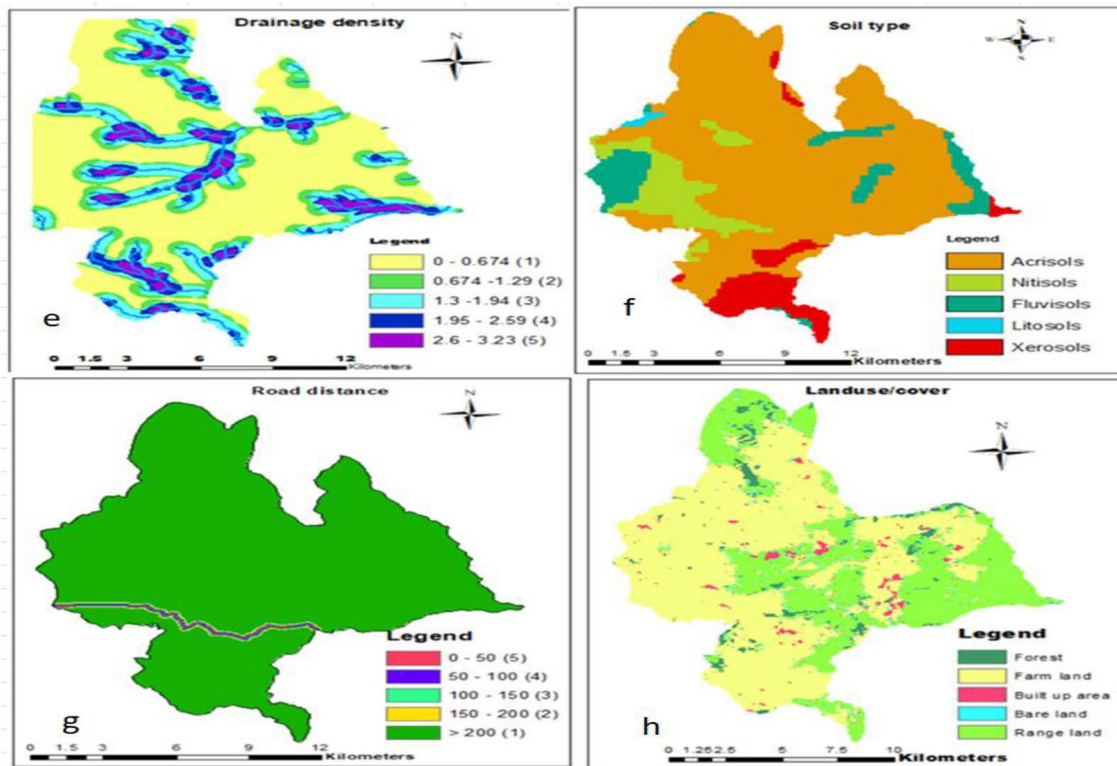


Fig. 4 Drainage density **e**, soil type **f**, road distance **g**, and land use/cover **h** Source, Reclassified map of the study area

Table 4 The pair-wise comparison matrix for selected landslide causative factors

Factors	Slope	Elevation	Aspect	Sd	Dd	St	Rd	LULC
Slope	1	2	3	2	2	3	2	2
Elevation	1/2	1	3	2	2	3	2	3
Aspect	1/3	1/3	1	2	2	1	1	2
Sd	1/2	1/2	1/2	1	2	2	3	2
Dd	1/2	1/2	1/2	1/2	1	2	2	3
St	1/3	1/3	1/2	1/2	1/2	1	2	2
Rd	1/2	1/2	1/2	1/3	1/2	1/2	1	2
LULC	1/2	1/3	1/2	1/2	1/3	1/2	1/2	1
Sum	4.17	5.50	10.50	8.83	10.33	13.00	14.00	17.00

Sd stream distance, Dd drainage density, St Soil type, Rd Road distance, LULC Landuse/cover

visits, and prior experience of the researchers/using supervised classification techniques. Land use/cover classes were prepared in ArcMap 10.8. The result shows large proportion of the study area which accounts for 61% was categorized as areas with very high and high susceptibility to landslide hazards, while the rest is identified as moderate, low, and very low (Table 3 and Fig. 4h).

4 Discussion

Once the landslide causative factors map preparation and reclassification were completed and the result identified the AHP matrix-based techniques were applied to assign relative values for each causative factor. The rating involved a paired comparison of one factor over the other using [27] AHP factors comparison scale (Table 1) according to the relative importance of factors to develop a pairwise comparison matrix based on the decision of the experts (Table 4). Since expert

Table 5 Normalized Pairwise comparison matrix & calculated criteria weight for causative factors

Factors	Slope	Elevation	Aspect	Sd	Dd	St	Rd	LULC	Sum	CVW	CW (%)
Slope	0.24	0.3636	0.2857	0.2264	0.1935	0.231	0.1429	0.1176	1.8006	0.2274	23
Elevation	0.12	0.1818	0.2857	0.2264	0.1935	0.231	0.1429	0.1765	1.5576	0.2068	21
Aspect	0.08	0.0606	0.0952	0.2264	0.1935	0.077	0.0714	0.1176	0.9218	0.0818	8
Sd	0.12	0.0909	0.0476	0.1132	0.1935	0.154	0.2143	0.1176	1.0511	0.1234	12
Dd	0.12	0.0909	0.0476	0.0566	0.0968	0.154	0.1429	0.1765	0.8851	0.1213	12
St	0.08	0.0606	0.0952	0.0566	0.0484	0.077	0.1429	0.1176	0.6783	0.0883	9
Rd	0.12	0.0909	0.0952	0.0377	0.0484	0.039	0.0714	0.1176	0.6198	0.0889	9
LULC	0.12	0.0606	0.0476	0.0566	0.0323	0.039	0.0714	0.0588	0.4858	0.0622	6

CVW criteria value weights, CW criteria weigh

Table 6 Calculated consistency of pairwise comparison (0.08)

Factors	Slope	Elevation	Aspect	Sd	Dd	St	Rd	LULC	WS	CW	WS/CW
Slope	0.2274	0.4136	0.2454	0.2468	0.2426	0.2649	0.1778	0.1244	1.9429	0.2274	8.54
Elevation	0.1137	0.2068	0.2454	0.2468	0.2426	0.2649	0.1778	0.1866	1.6846	0.2068	8.15
Aspect	0.0758	0.0689	0.0818	0.2468	0.2426	0.0883	0.0889	0.1244	1.0175	0.0818	12.44
Sd	0.1137	0.1034	0.0409	0.1234	0.2426	0.1766	0.2667	0.1244	1.1917	0.1234	9.66
Dd	0.1137	0.1034	0.0409	0.0617	0.1213	0.1766	0.1778	0.1866	0.982	0.1213	8.1
St	0.0758	0.0689	0.0818	0.0617	0.0607	0.0883	0.1778	0.1244	0.7394	0.0883	8.37
Rd	0.1137	0.1034	0.0818	0.0411	0.0607	0.0442	0.0889	0.1244	0.6581	0.0889	7.4
LULC	0.1137	0.0689	0.0409	0.0617	0.0404	0.0442	0.0889	0.0622	0.5209	0.0622	8.37

$\lambda_{\max} = 8.88$

WS weighted sum, CW criteria weight

judgment is a better tool for identifying and characterizing landslide susceptibility factors [27, 45] also highlight the importance of normalization in pairwise comparison as part of the AHP technique for landslide susceptibility assessment.

Subsequently, the normalization of the pairwise comparison matrix and the weight of each factor were calculated (Table 5) and a consistency check was executed (Table 6). The calculated weight/contribution of each causative factor (Table 5) for the susceptibility of landslide in the study area are (slope (23%), elevation (21%), aspect (8%), stream distance, and drainage density each (12%), soil type and road distance each (9%) and LULC (6%). After the computation of weight for each landslide causative factor, the Consistency Index (CI) and Consistency Ratio (CR) were calculated using (Eqs. 1, 2), respectively and the CI of 0.13 was calculated with the CR ratio of 0.08. To compute the CI, the calculated highest eigenvalue of the ($\lambda_{\max} = 8.88$) and the number of factors ($n = 8$) were employed and the Random Index (RI) of 4.41 suggested for the eight causative factors was obtained from the RI random table. The calculated value of the CR ratio is 0.08% which is found acceptable to use the comparison for weighted overlay analysis as it is less than 0.1% (Eq. 2) and used to produce a landslide vulnerability map of the study area. Though there is no universally accepted threshold, a higher Random Index value indicates a higher level of agreement among experts to be tolerable [19, 46].

A comparison with similar studies reveals that the identified criteria weights align with the consensus on the key factors influencing landslide susceptibility. For instance, studies conducted by [4] in mountainous regions with similar geological and topographic characteristics have consistently highlighted slope as one of the most influential factors in landslide occurrence. The relatively high weight assigned to the slope (23%) in our study is consistent with these findings, underscoring its critical role in determining landslide susceptibility.

Similarly, elevation has been widely recognized as a significant factor affecting landslide occurrence, particularly in hilly or mountainous terrains. The substantial weight attributed to elevation (21%) in our study aligns with previous research, emphasizing its importance in assessing landslide vulnerability. Aspect, stream distance, and drainage density have also been identified as important determinants of landslide susceptibility [1, 31, 34]. The proportional weights assigned to these factors (8%, 12%, and 12% respectively) are in line with existing literature, corroborating their influence on landslide occurrence. Moreover, soil type, road distance, and land use are recognized as crucial factors affecting the stability of slopes and the potential for landslide initiation in the study area.

Fig. 5 Landslide vulnerability map of the study area

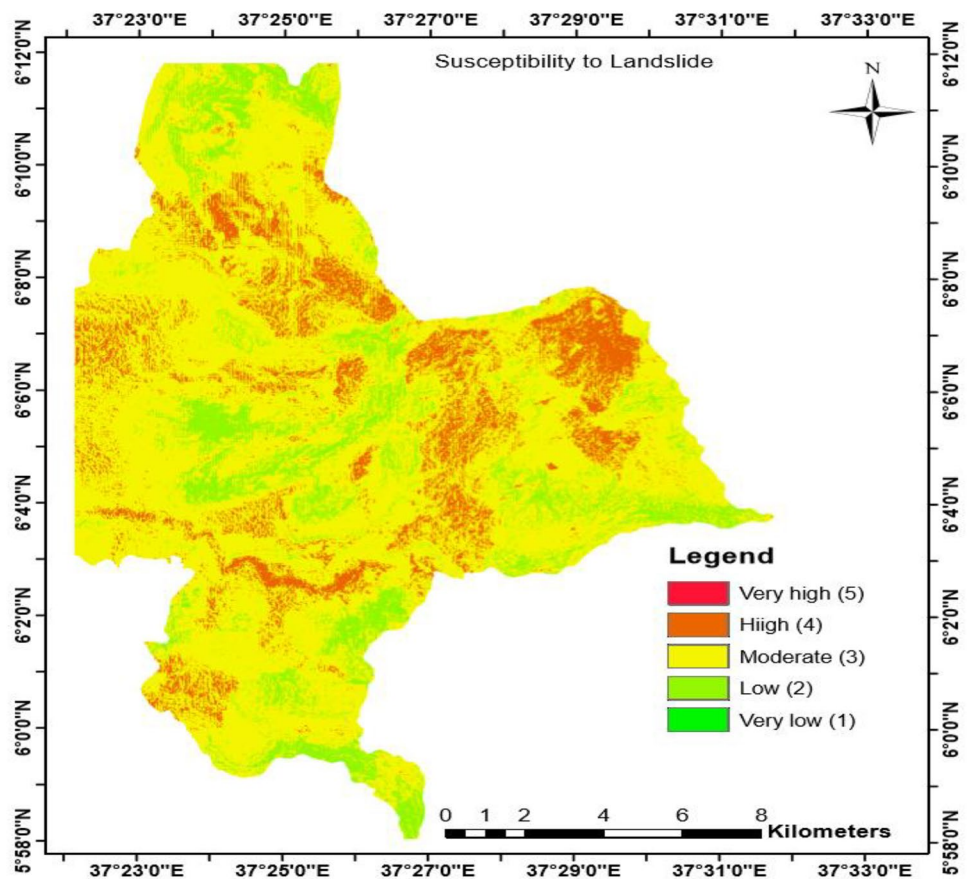


Table 7 Landslide vulnerability level, area coverage, and percentage

Landslide vulnerability level	Area	
	Hector	Percent
Very low (1)	0.04	0.4
Low (2)	2874.04	13
Moderate (3)	15,724.36	74
High (4)	2623.68	12
Very high (5)	0.06	0.6

4.1 Landslide vulnerability map of the study area

The final thematic landslide vulnerability map of the study area was prepared by the integration of eight causative factors (Fig. 5). Using the AHP and WLC method, the study district was categorized into five landslide vulnerability classes; very high (5), high (4), moderate (3), low (2), and very low (1). The estimated area of each susceptibility class was calculated (Table 7).

The prevalence of very high to moderate susceptibility classes covering [45] of the study district is consistent with observations from other research in analogous regions such as [19, 36] results suggest a significant level of vulnerability to landslides across the area, highlighting the urgency of implementing mitigation and preparedness measures. The relatively small proportion of the study area falling within very low and low vulnerability classes (13.4%) underscores the widespread susceptibility to potential landslide events, emphasizing the need for targeted risk reduction strategies.

Across the study sites, landslide susceptibility areas with very high to moderate vulnerabilities exist along the road crossing the district, high elevation areas, bare land, and agricultural lands found in the central, northeast,

east, and northwest of the study district particularly in the areas largely covered by acrisols soil types. Almost all the 11 villages in the district, namely, Gatse, Koddo, Wusamo, Zegiti Merche, Tsayite, Zegiti Bakole, Gerbenssa-Tsenkile, Kuyile, Lakka, Zegiti Peraso, and Mazo Doyisa are all identified within high to moderate landslide vulnerability class. More specifically, the five villages namely Gatse, Koddo, Wusamo, Zegiti Merche, and Tsayite fall within high and very high landslide vulnerability regions.

4.2 Validation of the model

There is a need for model validation to check the correctness of research output reality [37, 46, 48]. Thus, an effort was made to compare the model result with what was observed in the field. To validate the reliability of the output, the history of past landslide hazards that happened in the study district was collected from the sites with the help of the Global Positioning System (GPS) during fieldwork. The collected control points were overlaid on landslide susceptibility maps produced by the model, and it is confirmed by the past landslide history of the study area. Furthermore, the methodology employed in the study, using the AHP and WLC methods, is consistent with approaches commonly used in similar research [23, 41, 49] enhancing the credibility and reliability of the vulnerability classification. This reinforces the validity of the findings within the broader context of landslide vulnerability assessments.

5 Conclusion and recommendation

In this study, the Geographic Information System based Analytical Hierarchy Process and Weighted Linear Combination multi-criteria decision-making approach were employed to identify the status of landslide hazard in the Gacho Babba district of the Gamo zone. Eight causative factors for the landslide, namely, slope, elevation, aspect, distance from the stream, drainage density, soil type, distance from the road, and land use/cover were considered and their weightage values were determined based on the previous studies, an observation made during the fieldwork, experts judgment. The frequency of landslides in each of these causative factors was calculated using ArcGIS software spatial analysis tools and AHP matrix-based techniques. Subsequently, the normalization of the pairwise comparison matrix and the weight of each factor was calculated and consistency checks were executed. The calculated weight/contribution of each causative factor for the susceptibility of the study area for the landslide is (slope (23%), elevation (21%), aspect (8%), stream distance, and drainage density each (12%), soil type and road distance each (9%) and LULC (6%)). Lastly, after the computation of weight for each landslide causative factor, the Consistency Index (CI) and Consistency Ratio (CR) were calculated. The result shows that majorities which accounts (86.6%) of the study district falls within the very high to moderate landslide susceptibility class and only (13.4%) falls within very low and low vulnerability.

Based on the study results, it is recommended that urgent measures be implemented to mitigate and prepare for potential landslide events in the study district. The high prevalence of very high to moderate susceptibility classes suggests a significant level of vulnerability to landslides across the area. Therefore, targeted risk reduction strategies should be prioritized to address the widespread susceptibility to potential landslide events. Overall, the results indicate a substantial and widespread susceptibility to landslides within the study area, emphasizing the critical importance of proactive measures to mitigate potential impacts. Therefore, authorities and stakeholders must prioritize and implement proactive measures based on the study's findings to minimize the potential impacts of landslide hazards in the region.

Acknowledgements The authors are thankful to the editors and reviewers.

Author contributions The first author has performed the study design, literature review, data collection, software analysis, result interpretation, and writing the first draft of the manuscript. The second and third authors screen and coach the work proposed by the first author acting as a tiebreaker or criticizing and editing the work.

Funding The authors have not disclosed any funding.

Data availability The datasets generated and/or analyzed during the current study are available from the corresponding author upon reasonable request.

Declarations

Ethics approval and consent to participate This article does not contain any studies with human participants or animals performed by any of the authors.

Consent for publications Not applicable.

Competing interests The authors have no competing interests to declare that are relevant to the content of this article.

Open Access This article is licensed under a Creative Commons Attribution 4.0 International License, which permits use, sharing, adaptation, distribution and reproduction in any medium or format, as long as you give appropriate credit to the original author(s) and the source, provide a link to the Creative Commons licence, and indicate if changes were made. The images or other third party material in this article are included in the article's Creative Commons licence, unless indicated otherwise in a credit line to the material. If material is not included in the article's Creative Commons licence and your intended use is not permitted by statutory regulation or exceeds the permitted use, you will need to obtain permission directly from the copyright holder. To view a copy of this licence, visit <http://creativecommons.org/licenses/by/4.0/>.

References

1. Bragognolo R, Silva J. Artificial neural network ensembles applied to the mapping of landslides susceptibility. *J Hydrol Stud.* 2020;184:104240. <https://doi.org/10.1016/j.catena.2019.104240>.
2. UNISDR. (2019). United Nations international strategy for disaster reduction. terminology on disaster risk reduction. https://www.unisdr.org/files/7817_UNISDRTerminologyEnglish.pdf
3. Vikrant P, Subir S. Economic impact of natural disasters: an empirical re-examination. *J Appl Econ Res.* 2019;13(1):109–39. <https://doi.org/10.1177/0973801018800>.
4. Brito M, Weber J, Filho L. Multi-criteria analysis applied to landslide susceptibility mapping. *Revista Brasileira de Geomorfol.* 2017;18(4):719–35. <https://doi.org/10.0502/rbg.v18i4.111>.
5. World Bank Group. (2019). Disaster risk management. <https://www.worldbank.org/en/topic/disasterriskmanagement/overview>
6. Alejandro C, Manuel E, Mendoza T, José L. A review of recent studies on landslide hazard in Latin America. *Phys Geogr.* 2021. <https://doi.org/10.1080/02723646.2021.1978372>.
7. Dame T, Karuturi V, Dessie N, Binyam T. A model-based flood hazard mapping in Itang District of the Gambella region Ethiopia. *Geol Ecol Landscapes.* 2022. <https://doi.org/10.1080/24749508.2021.2022833>.
8. Mahmoud S. A multi-criteria approach to develop flood susceptibility maps in arid regions of Middle East. *J Clean Prod.* 2018;196:216–29. <https://doi.org/10.1016/j.jclepro.2018.06.047>.
9. Martínek K, Verner K, Hroch T, Megerssa L. Main Ethiopian Rift landslides formed in contrasting geological settings and climatic conditions Hazards. 2021. *Nat Earth Syst Sci.* <https://doi.org/10.5194/nhess-21-3465-2021>.
10. Gemechu S, Amare B, Ketema A, Davide G. Geographic information system-based-multicriteria analysis of flooding hazard and risk in Ambo Town and its watershed, West shoa zone, oromia regional State. Ethiopia *J Hydrol Reg Stud.* 2020;27: 100659. <https://doi.org/10.1016/j.ejrh.2019.100659>.
11. Filagot M, Suryabhadgavan KT, Elias K. Landslide hazard zonation and slope instability assessment using optical and InSAR data: a case study from gidole town and its surrounding areas Southern Ethiopia. *Remote Sensing Land.* 2019;3(1):1–14. <https://doi.org/10.1523/gcj1.19030101>.
12. Meten M. Frequency ratio density, logistic regression, and weights of evidence modeling for landslide susceptibility assessment and mapping in Yanase and Naka Catchments of Southeast Shikoku. *Japan Hindawi J Eng.* 2023;1062388(1–14):14. <https://doi.org/10.1155/2023/1062388>.
13. Getachew N, Meten M. Weights of evidence modeling for landslide susceptibility mapping of Kabi-Gebro locality, Gundomeskel area. *Central Ethiopia Environ Dis.* 2021;8(1):2–22. <https://doi.org/10.1186/s40677-021-00177-z>.
14. Abija F, Nwosu J, Ifedotun I, Osadebe C. Landslide susceptibility assessment of Calabar, Nigeria using geotechnical, remote sensing, and multi-criteria decision analysis: implications for urban planning and development. *SDRP J Earth Sci Environ Stud.* 2019;4:774–88. <https://doi.org/10.25177/JESES.4.6.RA.617>.
15. Thi Ngo PT, Panahi M, Khosravi K, Ghorbanzadeh O, Kariminejad N, Cerda A, Lee S. Evaluation of deep learning algorithms for national scale landslide susceptibility mapping of Iran. *Geosci Front.* 2021;12(2):505–19. <https://doi.org/10.1016/j.gsf.2020.06.013>.
16. Ibrahim M, Mustafa Z, Balogun A, Indra S, Nur Ain A. Landslide's analysis and Hazard mapping based on the analytic hierarchy process (AHP) using GIS, in Lawas Sabah-Sarawak. *Earth Environ Sci.* 2022;1064(1): 012031. <https://doi.org/10.1088/1755-1315/1064/1/012031>.
17. IPCC. (2020). Climate change impacts, adaptation and vulnerability summary for policymakers. <https://www.ipcc.ch/report/ar6/wg2/>
18. Das S, Gupta A. Multi-criteria decision based geospatial mapping of flood susceptibility and temporal hydro-geomorphic changes in the Subarnarekha basin. *India Geosci Front.* 2021;12(5): 101206. <https://doi.org/10.1016/j.gsf.2021.101206>.
19. Maes J, Kervyn M, Hontheim A. Landslide risk reduction measures: a review of practices and challenges for the tropics. *Progress Phys Geogr Earth Environ.* 2017;41(1):030913331668934. <https://doi.org/10.1177/0309133316689344>.
20. Woldearegai K. Review of the occurrences and influencing factors of landslides in the highlands of Ethiopia. *Momona Ethiop J Sci (MEJS).* 2013;5(1):3–31. <https://doi.org/10.4314/mejs.v5i1.85329>.
21. Fikre G, Raghuvanshi TK, Tenalem A, Trufat H. Landslide hazard zonation in Ada Berga district, Central Ethiopia—A GIS-based statistical approach. *J Geoman.* 2015;9:25–38.

22. UNISDR. (2016). United Nations international strategy for disaster reduction annual report. <https://www.undrr.org/publication/unisdr-annual-report-2016>
23. Leulalem S, Tarun K, Matebie M. Landslide susceptibility mapping using frequency ratio model: the case of Gamo highland. South Ethiopia Arab J of Geosci. 2021;14(623):2–18. <https://doi.org/10.1007/s12517-021-06995-7>.
24. Hamza T, Raghuvanshi K. GIS based landslide hazard evaluation and zonation a case from Jeldu District, Central Ethiopia. J King Saud Univ-Sci. 2016;29:151–65. <https://doi.org/10.1016/j.jksus.2016.05.002>.
25. Raghuvanshi T, Negassa L, Kala P. GIS based grid overlay method versus modeling approach a comparative study for landslide hazard zonation (LHZ) in Meta Robi District of west Shewa Zone in Ethiopia. Egypt JR Sp Sci. 2015;8(2):235–50. <https://doi.org/10.1016/j.ejrs.2015.08.001>.
26. Getnet M, Filagot M. Assessment of landslide risk in Ethiopia: distributions, causes, and impacts. Instit Geophys Space Sci Astron Addis Ababa Univ Ethiopia. 2022. <https://doi.org/10.5772/intechopen.101023>.
27. Saaty W. The analytic hierarchy process-what and how it is used. Math Modell. 1987;9(3–5):16. [https://doi.org/10.1016/0270-0255\(87\)90473-8](https://doi.org/10.1016/0270-0255(87)90473-8).
28. CSA. National population statistics federal Democratic Republic of Ethiopia. Addis Ababa: Central Statistical Authority; 2007.
29. Cherie S, Ayele N. Landslide susceptible mapping using InSAR and GIS techniques: overview of Debresina Area Ethiopia. J Geol Geophys. 2021;10:988. <https://doi.org/10.21203/rs.3.rs-3254900/v1>.
30. Zézere J, Pereira S, Melo R, Oliveira S, Garcia R. Mapping landslide susceptibility using data-driven methods. Sci Total Environ. 2017;589:250–67. <https://doi.org/10.1016/j.scitotenv.2017.02.188>.
31. Asmelash A, Giulio B, Kifle W. GIS-based landslide susceptibility evaluation using analytical hierarchy process (AHP) approach: the case of Tarmaber District. Ethiopia Momona Ethiopian J Sci. 2019;11(1):14–36. <https://doi.org/10.4314/mejs.v11i1.2>.
32. Ikram H, Lahsen B, Abderahman M, Abdellah A. The prevention of landslides, using the analytic hierarchy process (AHP) in a geographic information system (GIS) environment in the Province of Larache. Morocco Geomat Environ Eng. 2022;16(2):77–93. <https://doi.org/10.7494/geom.2022.16.2.77>.
33. Paola R, Mauro R, Bruce D, Monika M, Fausto G. A review of statistically-based landslide susceptibility models. Earth Sci Rev. 2018;180:60–91. <https://doi.org/10.1016/j.earscirev.2018.03.001>.
34. Rozos D, Bathrellos G, Skilodimou H. Landslide susceptibility mapping northeastern part of Achaia prefecture using analytical hierarchical process and GIS techniques, bulletin of the geological society of Greece. Proc Int Congress Patras. 2008;3:1637–46.
35. Ashrafal I, Sanzida M, Mainil K, Atikul H, Yousuf G, Israt J, Syed H. Utilization of opensource spatial data for landslide susceptibility mapping at chittagong district of bangladesh an appraisal for disaster risk reduction and mitigation approach. Int J Geosci. 2017;8(4):577–98. <https://doi.org/10.4236/ijg.2017.84031>.
36. Hagos Y, Andualem T, Yibeltal M, Mengie M. Flood hazard assessment and mapping using GIS integrated with multi-criteria decision analysis in upper Awash River basin. Ethiopia Appl Water Sci. 2022;12(7):2–18. <https://doi.org/10.1007/s13201-022-01674-8>.
37. Lee S, Rezaie F. Data used for GIS-based flood susceptibility mapping. Data Geol Ecol Oceanogr Space Sci Polar Sci. 2022;41:1–15. <https://doi.org/10.1007/s13201-022-01772-7>.
38. Budimir M, Atkinson P, Lewis H. A systematic review of landslide probability mapping using logistic regression. Landslides. 2015;12:419–36. <https://doi.org/10.1007/s10346-014-0550-5>.
39. Van Westen C, Van Asch T, Soeters R. Landslide hazard and risk zonation: bulletin of engineering. Geol and the Env. 2006;65:167–84. <https://doi.org/10.1007/s10064-005-0023-0>.
40. Ajanaw N, Dessalegn W, Alazar S, Haile G. Potential flood-prone area identification and mapping using GIS-based multi-criteria decision-making and analytical hierarchy process in Dega Damot district, northwestern Ethiopia. Appl Water Sci. 2022;12:255. <https://doi.org/10.1007/s13201-022-01772-7>.
41. Bharat P, Keshab A, Binod P, Thakur S, Gandhiv K. Using geographic information system and analytical hierarchy process in landslide hazard zonation. Appl Ecol Environ Sci. 2013;1(2):14–22. <https://doi.org/10.12691/aees-1-2-1>.
42. Zzaman R, Nowreen S, Billah M, Islam A. Flood hazard mapping of Sangu River basin in Bangladesh using multi-criteria analysis of hydro geomorphological factors. J Flood Risk Manag. 2021;14(6):1–19. <https://doi.org/10.1111/jfr3.12715>.
43. Allafta H, Opp C. GIS-based multi-criteria analysis for flood-prone areas mapping in the trans-boundary Shatt Al-Arab basin. Iraq-Iran Geomat Nat Haz Risk. 2021;12(1):2087–116. <https://doi.org/10.1080/19475705.2021.1955755>.
44. Davide N, Martina C, Danilo G, Daniele G. Semi-automatic mapping of shallow landslides using free Sentinel-2 images and Google Earth Engine. Nat Hazards Earth Syst Sci. 2023;23(2625):2648. <https://doi.org/10.5194/nhess-23-2625-2023>.
45. Hesheng C, Yi He, Lifeng Z, Sheng Y, Wang Y, Yumin F, Yaoxiang L, Binghai G. A landslide extraction method of channel attention mechanism U-Net network based on sentinel-2A remote sensing images. Int J Digital Earth. 2023;16(1):552–77. <https://doi.org/10.1080/17538947.2023.2177359>.
46. Robert E, Dalia K, Thomas S. New global characterization of landslide exposure. Natural Hazard Earth Syst Sci. 2020;434:1–21. <https://doi.org/10.5194/nhess-2019-434>.
47. Hong H, Panahi M, Shirzadi A, Ma T, Liu J, Zhu A-X, Chen W, Kougiaris I, Kazakis N. Flood susceptibility assessment in Hengfeng area coupling adaptive neuro-fuzzy inference system with genetic algorithm and differential evolution. Sci Total Environ. 2018;621:1124–41. <https://doi.org/10.1016/j.scitotenv.2017.10.114>.
48. Dahl M, Mortensen L, Veihe A, Jensen N. A simple qualitative approach for mapping regional landslide susceptibility in the Faroe Islands. Nat Hazards Earth Syst Sci. 2010;10:159–70. <https://doi.org/10.5194/nhess-10-159-2010>.
49. Wei C, Zenghui S, Jichang H. Landslide susceptibility modeling using integrated ensemble weights of evidence with logistic regression and random forest models. Appl Sci. 2019;9(1):171. <https://doi.org/10.3390/app9010171>.